A HYBRID METHOD FOR DETERMINING THE RELUCTIVITY TENSOR COMPONENTS OF GOSS TEXTURED FERROMAGNETIC MATERIALS

Hans Vande Sande [(1)], François Henrotte [(1)], Ludo Froyen [(2)], Kay Hameyer [(1)]

[(1)] **Katholieke Universiteit Leuven, Dept. Electrical Engineering, Div. ELECTA**
Kasteelpark Arenberg 10, B-3001 Leuven-Heverlee, Belgium
e-mail: hans.vandesande@esat.kuleuven.ac.be

[(2)] **Katholieke Universiteit Leuven, Dept. Metallurgy and Materials Engineering, Div. A2P2**
Kasteelpark Arenberg 44, B-3001 Leuven-Heverlee, Belgium

Abstract **–** For anisotropic materials, the vectors representing the magnetic field and the flux density are not parallel with each other. When measuring the magnetization along a direction making an angle á with the magnetic easy axis, by means of a single sheet tester, only the component of *B* projected on that direction is measured. It is impossible to deduce the angle between *B* and *H* from such measurements. For ferromagnetic materials having a Goss-texture, like most transformer steels, the paper demonstrates a way to compute this angle a posteriori, by the combination of measurements with a physical anisotropy model.

I. INTRODUCTION

It is customary in computational electromagnetics to directly implement material characteristics under the form under which they are given by the steel factories. As the measurements of such characteristics involve generally only scalar quantities, their implementation as such in a magnetic field finite element program constitutes a 'de facto' generalisation, which is not backed by any arguments nor even mentioned. Measurements give only a partial view on the complex behaviour of matter (and in particular that of iron and steel). They need therefore to be interpreted in the context of the mechanisms in play at the microscopic level. The purpose of this paper is to propose such an interpretation in the case of the analysis of the anisotropy of laminated steels.

Single strip testers measure the components of both the magnetic flux density *B* [T] and the magnetic field strength *H* [A/m] along one fixed direction in a thin sheet of material. They can be used to assess the anisotropy of the material, by measuring the magnetization curves of a series of small strips, cut out of a metal sheet under various angles. The reluctivity ν [Am/Vs]

$$\nu = \frac{H}{B} \quad , \tag{1}$$

depends non-linearly on *B*. Fig. 1 shows the measured reluctivity curves for a conventional grain-oriented (CGO) steel, along several directions with respect to the rolling direction [7,8].

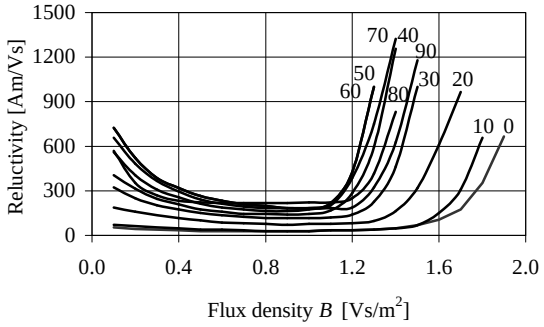

Fig. 1: The reluctivity curves for conventional grain-oriented steel, under various angles with respect to the rolling direction.

II. GOSS-TEXTURE

The curves plotted in Fig. 1 reveal the Goss-texture of the silicon steel. Silicon steel, mainly composed of cubic iron crystals, can be given a Goss-texture by an appropriate rolling process under specific conditions [3,6]. A silicon steel sheet features a Goss-texture if, for all crystals, the <001> axis coincides with the rolling direction and the {110} plane is parallel to the surface of the sheet (Fig. 2). From Fig. 1, it follows that the material is the most easily magnetized along the rolling direction (RD), while it is the hardest to magnetize at an angle of 54.7 ° with respect to the RD. This phenomenon is explicable by more thoroughly considering the magnetization process.

III. MAGNETIZATION PROCESS

All ferromagnetic materials are characterized by the presence of magnetic domains, in which the material is magnetized up to saturation magnetization M_s. For iron,

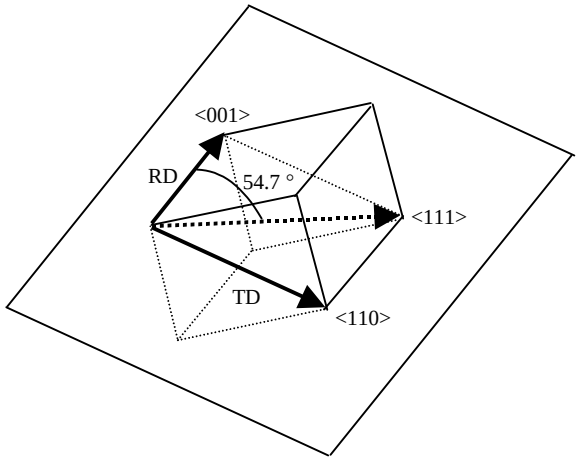

Fig. 2: Definition of a Goss-texture, with the rolling direction (RD) and the transverse direction (TD).

$M_s = 1.71 \cdot 10^6$ A/m [1]. If no external field is applied, these domains are randomly distributed with their magnetization vector along one of the preferred easy axes <100>, <010> or <001>. When the external field is increased slightly, the domains that are aligned in a direction close to that of the applied field start growing. At moderate fields, the domains suddenly and irreversibly rotate towards the easy axis that is the closest to the applied field. Once they are all parallel, i.e. above the knee of the magnetization curve, they rotate reversibly towards the applied field [1,2,3]. The latter process, also called coherent rotation, is described in terms of anisotropy and field energies. It explains the behavior observed in Fig. 1 at fields above 1T.

IV. ANISOTROPY AND FIELD ENERGY

The magnetization $\vec{M}_s$ [A/m] within a domain tends to align with one of the easy axes of the crystal. Each deviation from this equilibrium state corresponds to an increase of energy, which is due to the intrinsic anisotropy of the crystal. For cubic crystals, the anisotropy energy E_a [J/m^3] is given by

$$E_a = K_0 + K_1\left(\gamma_1^2\gamma_2^2 + \gamma_2^2\gamma_3^2 + \gamma_3^2\gamma_1^2\right) + K_2\left(\gamma_1^2\gamma_2^2\gamma_3^2\right) \quad , \quad (2)$$

with γ_1,γ_2 and γ_3 the direction cosines of $\vec{M}_s$ in the crystallographic coordinate system [7]. K_0 is an arbitrary constant. K_1 and K_2 are the anisotropy constants. In case of a cubic iron crystal, these are $K_1 = 0.48 \cdot 10^5$ J/m^3 and $K_2 = 0.05 \cdot 10^5$ J/m^3 [1]. On the other hand, if an external field $\vec{H}$ is applied, $\vec{M}_s$ tends to align with it. The corresponding energy E_h [J/m^3] is the so-called field energy

$$E_h = -\mu_0 \vec{M}_s \cdot \vec{H} \quad . \quad (3)$$

The process of coherent rotation of the domains can be considered as a competition between the anisotropy energy (2) and the field energy (3): $\vec{M}_s$ stabilizes in a direction for which the total energy is minimal.

For silicon iron having a Goss-texture, (2) and (3) simplify into

$$E_a = \frac{K_1}{4}\sin^2\theta\left(4 - 3\sin^2\theta\right) \quad (4)$$

and

$$E_h = -\mu_0 M_s H \cos(\alpha - \theta) \quad , \quad (5)$$

with α the angle between the field $\vec{H}$ and the RD, and θ the angle between $\vec{M}_s$ and the RD. The anisotropy energy (4) is plotted in Fig. 3. Obviously, $\theta = 54.7$ ° corresponds to a maximum of E_a. The field energy (5) is plotted in Fig. 4 for two values of H and α.

Figs. 5 and 6 show the total energy at low and high values for θ respectively. A cross indicates the location of the local minima. From these figures, it may be concluded that the magnetization vector takes up a position close to an easy axis, either $\theta \cong 0$ ° or $\theta \cong 90$ °, for fields up to 4000 A/m.

V. HYBRID MODEL

The hybrid method works in two steps. The direction of the magnetization M is first determined for a fixed direction of H, by means of the previous discussion. If $\alpha < 54.7$ °, the minimum of $E_a + E_h$ at low values of θ is determined. Else, the minimum for high values of θ is determined.

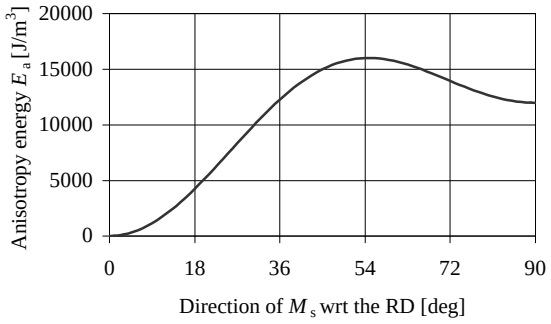

Fig. 3: The anisotropy energy for Goss-textured iron.

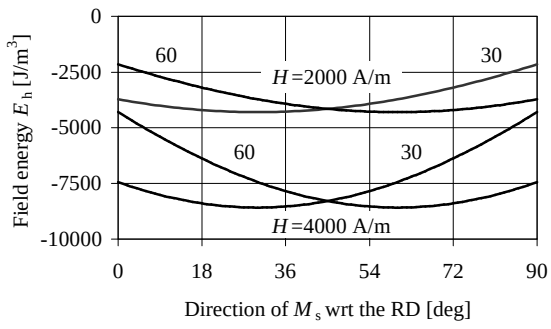

Fig. 4: The field energy for Goss-textured iron (α=30,60).

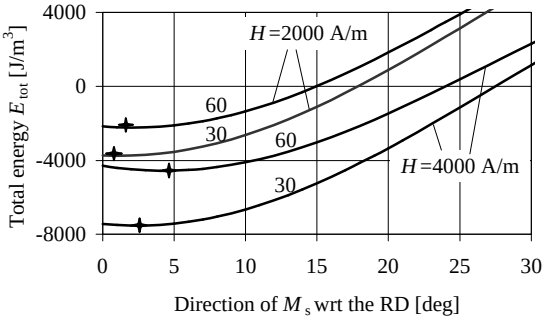

Fig. 5: The total energy for Goss-textured iron, at low θ (α=30,60).

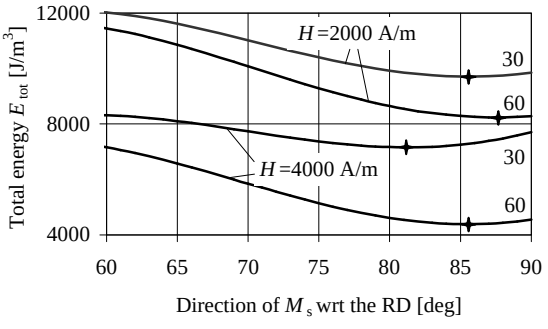

Fig. 6: The total energy for Goss-textured iron, at high θ (α=30,60).

The second step consists in extracting the amplitude of *M*, knowing its direction, from the single strip tester measurements. This is done as follows. The flux density *B* is related to the applied field *H* and the magnetization *M* by:

$$\vec{B} = \mu_0 \left(\vec{H} + \vec{M} \right) \quad . \tag{6}$$

Fig. 7 indicates how (6) is related to the single strip tester setup. By projecting (6) onto the direction á of the applied field, an expression for the amplitude of *M* is obtained:

$$M = \frac{\frac{B_{\text{meas}}}{\mu_0} - H}{\cos(\alpha - \theta)} \quad . \tag{7}$$

Subsequently, the components of *B* are obtained by projecting (6) on the RD and the TD:

$$\begin{cases} \frac{B}{\mu_0} \cos\beta = H \cos\alpha + M \cos\theta \\ \frac{B}{\mu_0} \sin\beta = H \sin\alpha + M \sin\theta \end{cases} , \tag{8}$$

with β the angle between *B* and the RD.

VI. RELUCTIVITY TENSOR

Using the previously presented hybrid approach, it is possible to compute the two components of *B* and hence the reluctivity tensor. If this symmetrical second order tensor is considered in its principal coordinate system, it has zero off-diagonal entries [4]. For this application, the RD and the TD are the principal axes of the tensor, as *B* and *H* are parallel in these directions. As a consequence

$$\begin{pmatrix} H_{\text{RD}} \\ H_{\text{TD}} \end{pmatrix} = \begin{pmatrix} \nu_{\text{RD}} & 0 \\ 0 & \nu_{\text{TD}} \end{pmatrix} \begin{pmatrix} B_{\text{RD}} \\ B_{\text{TD}} \end{pmatrix} \quad , \tag{9}$$

with

$$\nu_{\text{RD}} = \frac{H \cos\alpha}{B \cos\beta} \qquad \nu_{\text{TD}} = \frac{H \sin\alpha}{B \sin\beta} \tag{10}$$

for the specified measurement point.

VII. DATA SET

Now, the analysis is applied to an empirical data set, which matches the observed anisotropic behavior. For that, it is supposed that the Fröhlich-Kennely relation gives the shape of all magnetization curves [1,3]:

$$M = M_s \frac{\zeta H}{1 + \zeta H} \quad . \tag{11}$$

Depending on the magnetization angle, the flux density is multiplied by a factor, which expresses the fact that the magnetization is the easiest in the RD, that it is harder for the

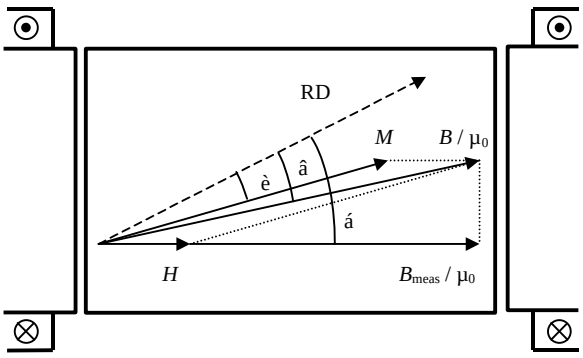

Fig. 7: The RD, *H*, *M* and *B* within the measurement setup.

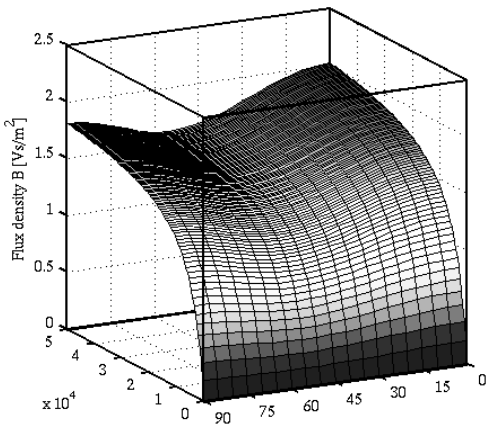

Fig. 8: The magnetization curves applied to explain the model.

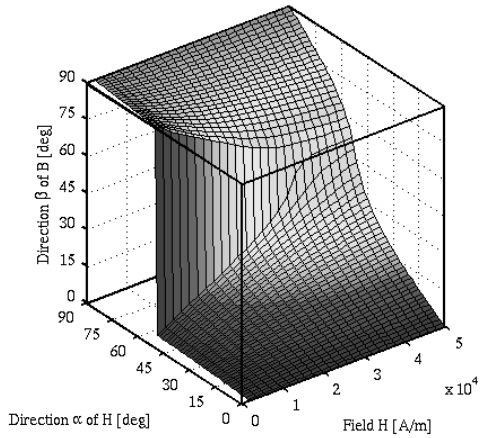

Fig. 9: The direction of *B*, for the data of Fig. 8.

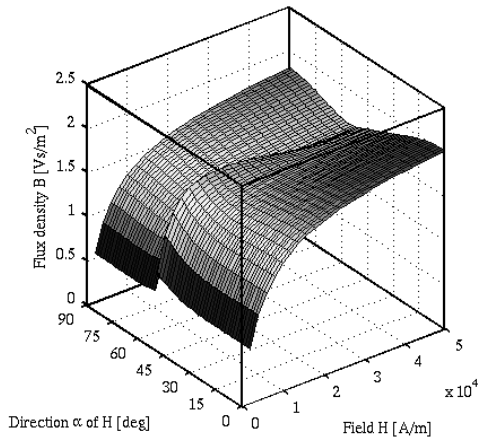

Fig. 10: The amplitude of *B*, for the data of Fig. 8.

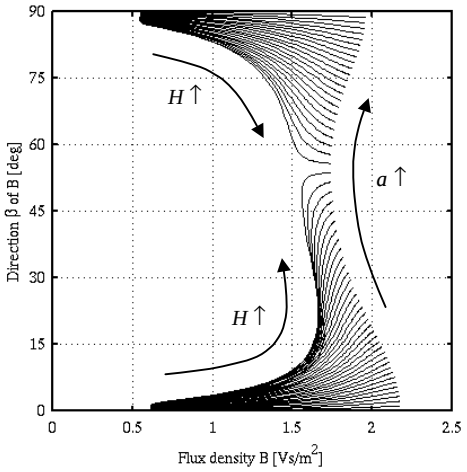

Fig. 11: Lines of constant α in the B-β plane, with parameter H, for the data of Fig. 8.

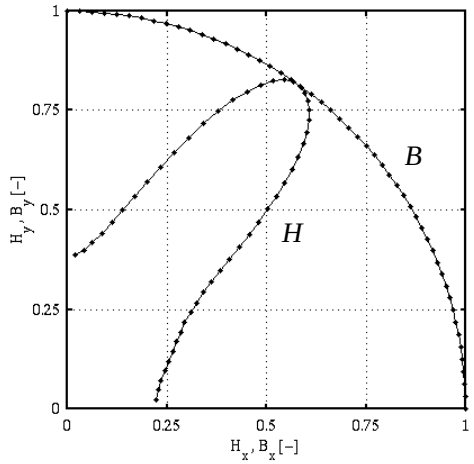

Fig. 12: The resulting H-locus, when B rotates with constant amplitude 1.7 T, for the data of Fig. 8.

TD and that it is the hardest for $\alpha = 54.7$ °. Moreover, the analysis is performed for higher fields than those used for measuring Fig. 1, in order to demonstrate the high field characteristics. The applied $B(H,\theta)$ model is plotted in Fig. 8, with $\zeta = 2 \cdot 10^{-4}$.

VIII. ANALYSIS

For the data set of Fig. 8, the computed direction β and the resulting flux density B are shown in Figs. 9 and 10 respectively. Obviously, Fig. 9 shows that for low fields H, the flux density vector stays close to the RD or the TD, irrespective of the field direction α. On the other hand, for higher fields, H and B tend to align. This is in correspondence with the theory of magnetization [1,2,3].

Fig. 10 reveals that, for a constant H, the actual amplitude of B does not behave like its measured component. The discontinuity which occurs for $\alpha = 54.7$ ° indicates that the total energy function has two local minima for low fields. This reveals an interesting feature, as B may point in two different directions for that angle. Hence, B must feature different behavior for right-turning fields than for left-turning fields, once α passes 54.7 °. The measurements with a single strip tester do not allow analyzing that type of behaviour. However, if Fig. 9 and Fig. 10 are combined, with H and α as a parameter, it can be observed that there is a large empty region in the B-β-plane (Fig. 11). In order to flip over the 54.7 °-direction, B must follow the contour of the empty region in a particular way. Fig. 11 also reveals how the field behaves, if the flux density rotates in space with constant amplitude. The result, for $|B| = 1.7$ T is plotted in Fig. 12, but it can be generalized to arbitrary B-loci in space. This will be considered in future research.

CONCLUSIONS

Single strip testers only measure the components of B and H in a single direction. Hence, in order to assess the magnetic anisotropy of a material, the magnetization curves must be measured in various directions. However, this does not yield any information about the instantaneous angle between $B(t)$ and $H(t)$. For Goss-textured ferromagnetic materials, a hybrid method is described that allows computing this angle. The direction of M is determined by minimizing the sum of anisotropy and field energy. Its amplitude is subsequently obtained from the measurements. The computation of the reluctivity tensor is then straightforward. The method is applied to an empirical data set. It is demonstrated that anisotropy may lead to a different behavior against low fields rotating in opposite directions. The method permits to determine the B-locus in space, given a H-locus and vice versa.

ACKNOWLEDGEMENTS

The authors are grateful to the Belgian "Fonds voor Wetenschappelijk Onderzoek Vlaanderen" (project G.0420.99) and the Belgian Ministry of Scientific Research (IUAP No. P4/20)

REFERENCES

[1] D. Jiles, Introduction to Magnetism and Magnetic Materials. London, UK, Chapman & Hall, 1991.

[2] P. Robert, Traité d'Electricité, Matériaux de l'Électrotechnique. Lausanne, Switzerland, Presses Polytechniques Romandes, 1987.

[3] R.M. Bozorth, Ferromagnetism. Princeton, New Jersey, D. Van Nostrand Company, 1951.

[4] J.F. Nye, Physical Properties of Crystals. Oxford, UK, Clarendon Press, 1985.

[5] M. Enokizono, "Two-dimensional (vector) magnetic property and improved magnetic field analysis for electrical machines", *Journal of Materials Processing Technology*, Vol. 108, pp. 225-231, 2001.

[6] D.N. Lee, H.T. Jeong, "The evolution of Goss texture in silicon steel", *Scripta Materialia*, Vol. 38, No. 8, pp. 1219-1223, 1998.

[7] G.H. Shirkoohi, M.A.M. Arikat, "Anisotropic properties in high permeability grain-oriented 3.25% Si-Fe electrical steel", *IEEE Trans. on Magnetics*, Vol. 30, No 2, pp 928-930, March 1994.

[8] G.H. Shirkoohi, J. Liu, "A finite element method for modelling of anisotropic grain-oriented steels", *IEEE Trans. on Magnetics*, Vol. 30, No 2, pp 1078-1080, March 1994.